(IJUSE) 2026, Vol. No. 13, Issue 1, Jan-Dec **e-ISSN: 2454-759X, p-ISSN: 2454-7581**

Kinetic And UV-Vis Spectroscopic Study of Azo-Chalcone Dye Formation from (E)-1-(4-Nitrophenyl)-3-Phenylprop-2-En-1-One with a Diazotized Reagent a DFT Computational Approach

Ahmed Hussein Ali Mohsin

University of Mosul, College of Education for Pure Science, Department of Chemistry, Mosul, 41002, Iraq.

[1]*Date of Receiving: 27 January 2026; Date of Acceptance: 18 February 2026; Date of Publication: 10 March 2026*

Abstract

The kinetics of azo-chalcone dye formation from (E)-1-(4-nitrophenyl)-3-phenylprop-2-en-1-one and diazotized 4-aminobenzoic acid were investigated. Chalcones exhibit valuable biological and optical properties, yet the kinetic parameters governing their azo-coupled derivatives remain incompletely characterized. This study aimed to determine the reaction rate constants, activation energy, and half-life for azo-chalcone dye formation under varying temperatures, and to validate the experimental findings using density functional theory (DFT) calculations. UV-Vis spectroscopy monitored the dye formation at 346 nm over 130 min at four temperatures (275, 285, 295, and 305K) under natural pH and optimized 1:10 stoichiometric ratio (Chalcone reagent). Pseudo-first-order kinetic analysis and the Arrhenius equation were applied. DFT calculations using the B3LYP/6-31G method were performed with Gaussian 09. The reaction followed pseudo-first-order kinetics (R^2 = 0.9627 – 0.9887). The rate constant increased from 0.0529 min^{-1} at 275K to 0.0616 min^{-1} at 305K, with corresponding half-life decreases from 13.1 to 11.3 min. Arrhenius analysis yielded an exceptional linear correlation (R^2 = 0.9999) and an activation energy of 3.54 kJ mol^{-1}. DFT calculations identified nitrogen and oxygen atoms as the primary donor-active sites. The temperature-dependent kinetic behavior aligns with literature on azo-imine dye formation, indicating a low energy barrier and minimal thermal sensitivity for the pseudo-first-order proces. DFT validation supports the spectroscopic observations and elucidates the electronic properties governing reactivity. The azo-chalcone dye formation follows pseudo-first-order kinetics under the optimized conditions. The rate constants increase with temperature, and DFT confirms the reaction mechanism. These findings contribute to understanding azo dye synthesis for potential biological and optical applications.

Keywords: *azo-chalcone; density functional theory; kinetics; UV-Vis spectroscopy.*

INTRODUCTION

Chalcones are effective aromatic compounds and are the origin of various precursors or molecules in medicine [1 - 3]. They are useful as intermediates in the synthesis of various biologically active heterocyclic compounds. [3], such as pyrazolines [4 - 6] and isoxazoles [7 - 8]. The parent chalcone has the IUPAC name (1,3-diphenyl-2-propen-1-one), and other names such as benzylidene acetophenone, phenyl styryl ketone, Benza acetophenone, alpha-phenyl-β-benzoyl ethylene, fruits, vegetables, spices, and tea [9]. Chalcones are the most abundant natural compounds in soybean foods and have been extensively studied for many years due to their interesting pharmacological actions [10]**.** Chalcone skeletons are found in many natural products and exhibit valuable biological properties, such as antioxidant activity against protein damage. In contrast to cancer, cardiovascular, and

[1] *How to cite the article:* Mohsin A.H.A.; (March 2026); Kinetic And UV-Vis Spectroscopic Study of Azo-Chalcone Dye Formation from (E)-1-(4-Nitrophenyl)-3-Phenylprop-2-En-1-One with a Diazotized Reagent a DFT Computational Approach; *International Journal of Universal Science and Engineering;* Vol 13, 20-33

neurological diseases, which have widespread use as anti-inflammatories, antihistamine, anticancer, antimalarial **[**11 **-** 14**]**. Antiviral, bactericidal, antioxidant, and antidiabetic agents are used, along with the well-known chalcone compounds now available on the market. Many researchers have investigated the evaluation and rape of several chalcone compounds as anticancer agents [15 - 18**].** Apart from chemistry, the fluorescence of chalcones upon activation of an electron-donating group on the aromatic ring is well known and can be used as a probe to elucidate the mechanism [1]. Chalcone derivatives exhibit nonlinear optical (NLO) properties. characterized by good blue light transmission and excellent crystallinity. Optics concerns not only integrated optics and electronics but also the interfaces between optical materials, devices, and systems. The discovery of nonlinear optical (NLO) lasers has opened many new areas of real interest to humanity, such as frequency conversion and optical switching. The Claisen-Schmidt condensation reaction (aldol condensation) is the simplest method for generating a functional group [19 - 21**]**. The synthesis of compounds from the combination of two or more natural products results in insoluble molecules with multiple structures. The goal of such synthesis is to predict the chemical properties of two or more biologically active molecules that have combined to enhance these activities or to obtain derivatives exhibiting novel properties. Anticancer, it has been reported to exhibit various biological activities, including antioxidant and hypertensive activities **[**22 - 23]. Structures of different synthetic compounds were assigned based on elemental analysis, IR, and 1H NMR spectral data [24]. At this stage, computational chemistry becomes an indispensable tool in modern chemical science. For example, density functional theory (DFT) allows for the precise determination of quantum chemical parameters, including the energy of the lowest unoccupied molecular orbital (ELUMO), the energy of the highest occupied molecular orbital (EHOMO), the energy gap ($\Delta E = E_{LUMO} - E_{HOMO}$), Fukui indices, and the dipole moment (μ). This quantum parameter is directly related to a molecule's reactivity. Molecular dynamics (MD) simulations deepen to understand the global chemical reactivity and kinetic stability of the synthesized dye. The frontier molecular orbital energies ($EHOMO_)$ and ($ELUMO_)$ were evaluated to understand the global chemical reactivity and kinetic stability of the synthesized dye, reflecting its electron-donating and electron-accepting capabilities during the reaction.

The main objective of this study was to conduct a detailed spectroscopic investigation of the kinetic reactions involved in the synthesis of colored azo chalcones. These are derived from electron-donating elements, e.g., 1-(4-nitrophenyl)-3-phenyl prop-2-en-1-one. with its respective diazotized reagent, in the presence of 4-amino benzoic acid, which accepts these electrons under natural conditions as a function of pH and a specific temperature 295 K. Furthermore, the evidence was strengthened by a theoretical study that helped reduce effort, cost, and pollution.

EXPERIMENTAL

Materials and equipment

All starting chemicals and reagents were purchased from commercial suppliers (Fluka) and (BDH) and utilized without further purification. The chemical materials used in this study include: sodium hydroxide [CAS 1310-73-2], acetophenone [CAS 98-86-2], benzaldehyde [CAS 100-52-7], ethanol [CAS 64-17-5], 4-aminobenzoic acid [CAS 150-13-0], hydrochloric acid [CAS 7647-01-0], sodium nitrite [CAS 7632-00-0], and sodium carbonate [CAS 497-19-8]. Distilled water was used exclusively for preparing all aqueous solutions.

The experimental instrumentation comprised the following equipment:

1-Shimadzu UV-1800 (Double-Beam UV-Visible Spectrophotometer) TCC-100 Thermoelectrically-Temperature-Controlled Cell Holder.

2- pH-meter (JENWAY 3510).

3-Melting point 30 SMP-2003 Bibby Scientific Limited.

Table (1): The aromatic compounds being studied, complete with their numerical identifiers, symbolic representations, nomenclature, and certain physical characteristics, in addition to their inherent structural framework.

No.	Symbol of Derivative	Name	Structure	Molecular Formula	M.wt (gm.mol^{-1})
1-	E14NP3PP2E1O	(E)-1-(4-nitrophenyl)-3-phenylprop-2-en-1-one	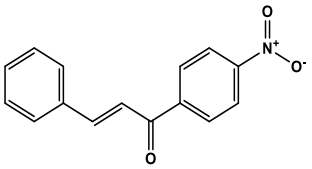 (*E*)-1-(4-nitrophenyl)-3-phenylprop-2-en-1-one	$C_{15}H_{11}NO_3$	253.26
2-	D4AbzA	Diazotized-reagent (4-Amino Benzoic acid)	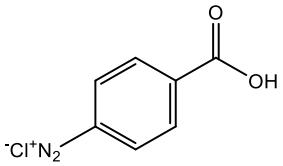 Molecular Weight: 184.58	$C_7H_5N_2O_2^+Cl^-$	184.58
3-	E14NP3PP2E1O + D4AbzA	4-((Z)-(3-((E)-3-(4-nitrophenyl)-3-oxoprop-1-en-1-yl) phenyl) diazenyl) benzoic acid	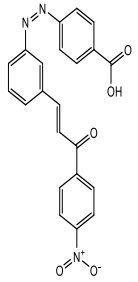 4-((*Z*)-(3-((*E*)-3-(4-nitrophenyl)-3-oxoprop-1-en-1-yl)phenyl)diazenyl)benzoic acid	$C_{22}H_{15}N_3O_5$	401.38

Synthesis of Chalcone Derivative (E14NP3PP2E1O)

A 0.01 M portion of acetophenone was mixed with 5 mL of a 10 percent w/v aqueous sodium hydroxide solution. The mixture was dissolved in 5 mL of ethanol and subjected to continuous stirring for approximately 30 min. Subsequently, a 0.01 M amount of benzaldehyde dissolved in 5 mL of ethanol was introduced dropwise into the reaction mixture. Stirring was maintained at room temperature for 2 h. The resulting crude product was collected, washed thoroughly with cold distilled water until a neutral pH was achieved, dried, and purified via recrystallization from ethanol [9].

Preparation of diazotized reagent solution (D4AbzA):

The diazotized reagent was prepared by dissolving 0.0462 g of 4-aminobenzoic acid in 50 mL of distilled water, followed by the addition of 20 mL of 1 M hydrochloric acid [25]. The mixture was gently warmed to ensure complete dissolution and then transferred to an ice bath to cool between 0 to 5 degrees Celsius. Under vigorous stirring, 8.65 mL of a chilled 1 percent w/v sodium nitrite solution was added dropwise. The mixture was allowed to stir for an additional 5 min [26]. The final diazonium salt solution was diluted with cold distilled water and stored in a black-coated glass container shielded from light to prevent thermal or photochemical decomposition, Equation 2.

Eq.1.

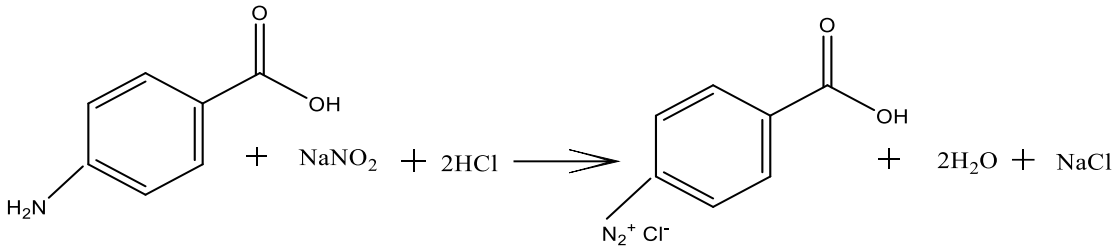

Eq.2.

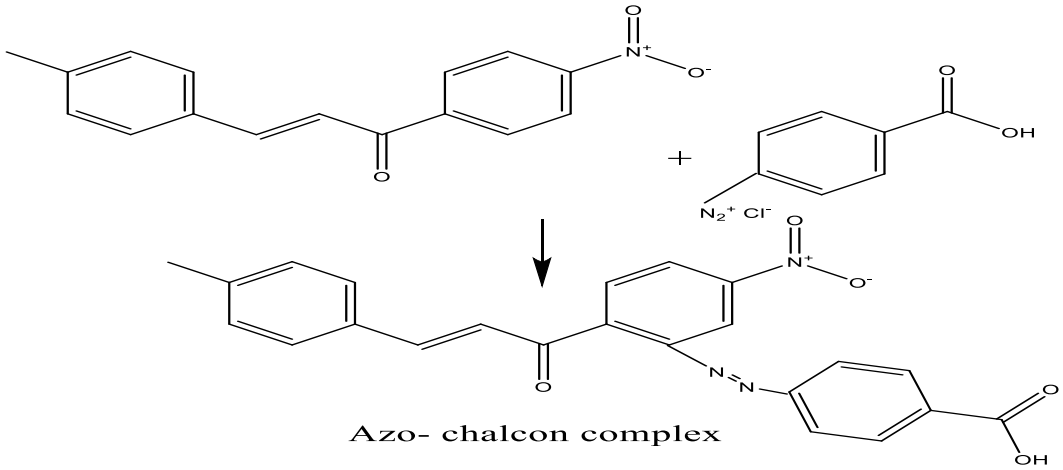

Kinetic measurements:

All kinetic experiments for the coupling reaction between the synthesized chalcone and the reagent were performed using a Shimadzu UV-1800 spectrometer. The cell carrier temperature was precisely controlled and maintained to an accuracy of ± 0.1 C° throughout each experiment. The absorption of the reaction mixture was continuously monitored at the maximum wavelength (λ_{max}) at regular intervals for a total of 130 minutes to ensure the reaction reached its maximum conversion [27].

Table 2: Spectroscopic and physicochemical properties of the synthesized azo-chalcone dye.

No.	The symbol	pH	Absorbance	λ_{max} (nm.)
1-	E14NP3PP2E1O	7.4	1.412	334
2-	D4AbzA	1.95	0.922	294
3-	E14NP3PP2E1O + D4AbzA	5.61	1.532	346

(IJUSE) 2026, Vol. No. 13, Issue 1, Jan-Dec **e-ISSN: 2454-759X, p-ISSN: 2454-7581**

Table 2 clearly shows that there is no interaction between the resulting azo-chalcone dye solution and the reagent solution.

To monitor azo dye formation, the reaction was performed under optimized conditions at the ideal maximum wavelength ($\lambda_{max)}$**.** Spectroscopic analysis showed no side interactions between the generated dye and the components of the initiating reaction. The kinetics of product formation were then evaluated using a first-order theoretical kinetic equation. a 130-min tracking period. These kinetic results are illustrated in the accompanying chart and diagram.

This is also supported by the varying half-lives observed in dye formation at different temperatures. The study used the integration method to monitor the kinetics of colored dye formation. By applying the pseudo-first-order equation to the collected kinematic data, we could investigate reaction kinetics.

$Ln\{A_\infty/(A_\infty-A_t)\}= k1.t$ ----------(Eq. 1)

Plotting a graph of Ln{A∞/(A∞-At)} against time (in minutes) yielded straight lines at all four temperatures with ($R^{2)}$ values ranging from 0.9627 to 0.9887. The slopes of these lines correspond to the velocity constants ($k_{1)}$ for the formation reactions, indicating that the dye's formation reaction follows a pseudo-first-order mechanism, as with the chalcone. Using these values, we determined the velocity constant of the dye at 275, 285, 295, and 303K. This allowed us to calculate the corresponding half-life times (t1/2) using Equation 2.

$t_{1/2}$=Ln2.0/k_1----------(2)

($t_{1/2}$=11.3minutes at 305K), ($t_{1/2}$=11.8minutes at 295K), ($t_{1/2}$=12.4minutes at 285K), ($t_{1/2}$=13.1minutes at 275K).

Table (3): Monitoring the absorption of the resulting colored Azo-Chalcone-dye (E14NP3PP2E1O+ D4ABzA) versus time (minutes) at different temperatures, at natural pH, and at the optimum wavelength (λ_{max} = 346nm).

Temperatures (°K)															
Absorbance				$A_\infty-A_t$				$A_\infty/(A_\infty-A_t)$				LN($A_\infty/(A_\infty-A_t)$)			
305	295	285	275	305	295	285	275	305	295	285	275	305	295	285	275
0.000	0.000	0.000	0.000	1.566	1.546	1.528	1.511	1.0	1.0	1.0	1.0	0.00	0.00	0.00	0.00
0.303	0.292	0.289	0.276	1.264	1.255	1.240	1.236	1.2	1.2	1.2	1.2	0.21	0.21	0.21	0.20
0.633	0.612	0.61	0.561	0.935	0.936	0.919	0.952	1.7	1.7	1.7	1.6	0.52	0.50	0.51	0.46
0.824	0.806	0.803	0.792	0.744	0.741	0.727	0.720	2.1	2.1	2.1	2.1	0.74	0.74	0.74	0.74
0.908	0.902	0.896	0.889	0.659	0.645	0.633	0.623	2.4	2.4	2.4	2.4	0.87	0.87	0.88	0.89
1.107	1.103	1.097	1.085	0.461	0.445	0.433	0.427	3.4	3.5	3.5	3.5	1.22	1.25	1.26	1.26
1.201	1.193	1.190	1.184	0.367	0.355	0.339	0.330	4.3	4.4	4.5	4.6	1.45	1.47	1.51	1.52
1.268	1.264	1.261	1.256	0.299	0.283	0.269	0.256	5.2	5.5	5.7	5.9	1.66	1.70	1.74	1.78
1.386	1.322	1.320	1.315	0.181	0.225	0.209	0.197	8.7	6.9	7.3	7.7	2.16	1.93	1.99	2.04
1.390	1.372	1.367	1.360	0.178	0.175	0.162	0.152	8.8	8.8	9.4	9.9	2.17	2.18	2.24	2.30
1.463	1.402	1.399	1.389	0.107	0.145	0.129	0.123	15.1	10.7	11.8	12.3	2.71	2.37	2.47	2.51

1.505	1.458	1.456	1.417	0.062	0.089	0.073	0.096	25.3	17.4	20.9	15.7	3.23	2.85	3.04	2.76
1.515	1.514	1.479	1.438	0.051	0.032	0.051	0.074	30.7	48.3	30.0	20.4	3.42	3.88	3.40	3.02
1.519	1.517	1.482	1.456	0.048	0.029	0.047	0.060	32.6	53.3	32.5	25.2	3.49	3.98	3.48	3.23
1.528	1.523	1.490	1.468	0.039	0.024	0.039	0.045	40.2	64.4	39.2	33.6	3.69	4.17	3.67	3.51
1.552	1.527	1.506	1.489	0.015	0.020	0.023	0.023	104.4	77.3	66.4	65.7	4.65	4.35	4.20	4.19
1.559	1.536	1.515	1.493	0.009	0.011	0.014	0.019	174.0	140.5	109.1	79.5	5.16	4.95	4.69	4.38
1.560	1.537	1.517	1.502	0.007	0.010	0.012	0.010	223.7	154.6	127.3	151.1	5.41	5.04	4.85	5.02
1.562	1.540	1.522	1.511	0.005	0.007	0.007	0.000	313.2	220.9	218.3	∞	5.75	5.40	5.39	-
1.564	1.542	1.523	1.510	0.003	0.005	0.006	0.002	522.0	309.2	254.7	755.5	6.26	5.73	5.54	6.63
1.566	1.543	1.529	1.489	0.001	0.004	0.000	0.023	1566.0	386.5	∞	65.7	7.36	5.96	-	4.19
1.567	1.544	1.512	1.422	0.000	0.003	0.017	0.090	∞	515.3	89.9	16.8	-	6.24	4.50	2.82
1.562	1.545	1.489	1.392	0.005	0.002	0.040	0.120	313.2	773.0	38.2	12.6	5.75	6.65	3.64	2.53
1.540	1.547	1.314	1.309	0.027	0.000	0.215	0.203	58.0	∞	7.1	7.4	4.06	-	1.96	2.01
1.524	1.535	1.288	1.256	0.043	0.013	0.241	0.257	36.4	118.9	6.3	5.9	3.60	4.78	1.85	1.77
1.515	1.513	1.267	1.242	0.052	0.034	0.263	0.270	30.1	45.5	5.8	5.6	3.41	3.82	1.76	1.72
1.489	1.488	1.234	1.209	0.079	0.059	0.296	0.303	19.8	26.2	5.2	5.0	2.99	3.27	1.64	1.61

The highest absorbance (A∞), formation expiration times (t∞), formation rate-constants (k_1), and half-life-times (t1/2) for the colored Azo-Chalcone-dye formation were obtained at the four temperatures from Table 3. Figure 1 also shows that the rate constant varies across the four temperatures studied, leading to contrasting half-life values. As demonstrated in Table 4:

Table (4): The values of the highest absorbance(A_∞), their formation expiration times(t_∞), rate constants of their formation(k_1), and their half-life times ($t_{1/2}$), for the formation of the studied produced Azo-Chalcone-dye (E14NP3PP2E1O+ D4ABzA) at the four temperatures.

Temperatures (k)	t_∞ (min.)	A_∞	k_1 (min.$^{-1}$)	($t_{1/2}$) (min.)
305	105	1.566	0.0616	11.3
295	115	1.546	0.0587	11.8
285	100	1.528	0.0558	12.4
275	90	1.511	0.0529	13.1

Computational details

Quantitative chemistry calculations were performed using the (Gaussian.09) software package, while molecular structures were constructed and visualized using (Gauss View 6.0.16), which can perform composite geometry optimization in the presence of the solvent, using the density functional theory (DFT) method with the hybrid Beck function (B3LYP) at base set 6-31G. These values were used to deduce the electron affinity (A), ionization potential (I), and chemical hardness (η) [28, 29].

The engineering optimization of (E14NP3PP2E1O) was performed using the (DFT-B3LYP/6-31G) by (Gaussin.09) method. Both the occupied higher molecular orbital (HOMO) and the unoccupied lower molecular orbital (LUMO) are fundamental to understanding the molecular properties of (E14NP3PP2E1O). The (HOMO) of (D4ABzA) represents the electron-donating orbitals, while the (LUMO) represents the electron-accepting orbitals. This energy gap, Energy gap = (HOMO-LUMO), is crucial in determining the chemical stability and reactivity of the compounds; a high Energy gap value is associated with stability, while a low Energy gap value is associated with reactivity [48]. A low Energy gap indicates the ease of electron transfer from the (HOMO) of (D4ABzA) to the surface of (E14NP3PP2E1O), in contrast to a high Energy gap, which indicates that electron transfer from the (HOMO) to the surface orbital of (E14NP3PP2E1O) requires more energy. From the Energy gap value, other quantitative chemical parameters, such as Electronegativity, Chemical hardness, Electron affinity index, and Chemical softness, can be calculated using the equations presented by Shams et al [29]. These quantitative parameters, derived from density functional theory (DFT) methods, the compound was evaluated for its kinetic behavior and electronic properties to understand its reactivity and stability during the dye formation process. Table 5 shows the (HOMO) and (LUMO) values and the quantitative parameters, as well as the (HOMO) and (LUMO) plots for the studied compounds. The results show that all the compounds under investigation exhibited a high ionization potential (IP) [30]. All (DFT) calculations using the (Gaussian.09).

Table (5): Calculated HOMO, LUMO, Eg, and global descriptors for the (14NP3PP2E1O) & (D4ABzA) compound.

Compound	HOMO eV	LUMO Ev	Eg eV	μ (eV)	η (eV)	ω (eV)
E14NP3PP2E1O	-6.8099	-3.3404	3.4694	-5.0749	-1.7347	-7.4232
D4ABzA	-10.3566	0.9197	11.3308	-7.5430	-5.6654	-2.8054

Statistical analysis

All measurements were performed three times, and the average values were calculated. To determine the Regression Assumptions, correlation coefficient ($R^{2)}$ between the results obtained, a statistical analysis was performed using the professional statistical software (Minitab.18).

RESULTS

The experimental and theoretical data obtained from the kinetic tracking and computational investigation of the azo-chalcone dye formation are detailed in this section. All parameters were systematically recorded and calculated across the specified temperature range.

Kinetic data and rate constants

The absorbance changes during the dye coupling reaction were monitored at regular intervals up to 130 min. The calculated rate constants ($k_{1)}$ and the corresponding reaction half-life (t1/2) values for the pseudo-first-order process at different temperatures are presented in Table 3 and Table 4.

Activation Energy:

The temperature dependence of the rate constants was evaluated using the Arrhenius plot regression (Figure.2). The mathematical calculation yielded an experimental activation energy (Ea) of 3.54 kJ / mol for the azo-chalcone dye formation process.

Molecular Orbital Descriptors:

The quantum chemical parameters calculated via Density Functional Theory (DFT) at the (B3LYP 6-31G) d, p level is summarized in Table 5. The extracted electronic properties include the highest occupied molecular orbital energy ($EHOMO_{)}$, the lowest unoccupied molecular orbital energy ($ELUMO_{)}$, and the global chemical descriptors. The computed molecular Energy gap (Eg) for the synthesized dye structure was verified to be 3.47 eV.

DISCUSSIONS

Effect of temperature on reaction kinetics the increase in the (k_1) value from 0.0529 min^{-1} at 275 K to 0.0616 min^{-1} at 305 K shows that the higher temperature accelerates the formation of the azo-chalcone dye. The decrease in half-life from 13.1 to 11.3 minutes indicates that the reaction proceeds more quickly at higher temperatures.

1. Reaction mechanism: The linear relationship observed in plots of $Ln\{A\infty/(A\infty-At)\}$ versus time supports a pseudo-first-order kinetic model for the dye formation reaction. The reagent concentration was maintained at 10 times the chalcone concentration, and the researchers observed that, under these conditions, the reaction rate constant was unaffected by increasing the reagent concentration. To assess the reaction kinetics using a pseudo-first-order model, the linear regression was strictly limited to the initial upward phase of the reaction (from 0 to 90 minutes). After 90 minutes, a slight decrease in absorbance was experimentally observed. This decrease is attributed to the initiation of slow secondary degradation or slight deterioration of the dye complex formed under continuous exposure, causing a deviation from the ideal absorbance value ($A\infty$). Therefore, to maintain physical significance and avoid kinetic distortions, the ideal absorbance value ($A\infty$) was set at the highest stable absorbance value achieved at 90 minutes. The high correlation coefficient confirmed that the pseudo-first-order model accurately describes the dye formation process during this specific time frame before any degradation effects occur.

   The kinetic optimization revealed that employing a tenfold excess of the diazotized reagent concentration (5 mL of 10-3 M) relative to the phenyl chalcone substrate (0.5 mL of 10-3 M) resulted in a proportional tenfold increase in dye absorbance without causing side interactions. This specific stoichiometric ratio effectively maintains pseudo-first-order conditions, ensuring that the reaction rate depends solely on the chalcone concentration during the active coupling phase, as illustrated in the accompanying tracking trends [12].

2. Spectral and theoretical compatibility: UV and visible measurements showed the formation of an azo-chalcone dye at ($\lambda_{max)}$ = 346 nm. Density functional theory (DFT) calculations confirmed the spectroscopic observations by identifying donor nitrogen and oxygen atoms as the primary active centers in the reaction.

Furthermore, the quantum chemical calculations performed via density functional theory (DFT) indicated that the synthesized dye structure possesses a high ionization potential (IP), as extracted from the optimized theoretical frameworks. This theoretical threshold strongly underlines the intrinsic electronic stability of the conjugated organic chromophore, fully supporting the spectroscopic observations and confirming that the compound exhibits favorable electronic parameters under natural measurement environments [28-30] .

3. Activation energy**:** The calculated activation energy of 3.54 kJ/mol indicates an extremely low thermal barrier to dye formation. This experimental value is consistent with the small observed change in the reaction rate constants (k_1), which increase by only 16 % within the 30 K temperature range (275 K,285K,295K, and 305 K), resulting in a thermal coefficient (Q_{10}) of approximately 1.05 (p1).While typical chemical reactions exhibit higher activation energy (Ea) values, this extremely low activation energy suggests that the process is highly favorable and encounters virtually no kinetic barrier under the given conditions. Furthermore, the high linear correlation ($r^2 = 0.999$) is a mathematical consequence of the narrow variation in the dependent variable, confirming the high-reproducibility of the parallel data points, and not an indication of artificial accuracy (p1).

The graph in Figure 1 shows a clear relationship between the absorbance of the Azo-Chalcone dye and time under optimal conditions, at natural pH levels, and across different temperatures. It is worth noting that absorbance suddenly rises at specific time intervals across different temperatures. According to these points, the absorption plateaus once the dye-forming reaction is complete. These alterations do not affect the dye's λ max values, confirming that the reaction is complete [31-33].

4. Comparison with previous studies and stoichiometric effects: The experimental kinetic trends, temperature dependence, and half-life behaviors observed in this study are consistent with previous investigations on azo dye and azo-imine formation reactions [33-35]. Furthermore, the optimization of the reaction conditions indicated that maintaining a tenfold stoichiometric excess of the diazotized reagent concentration relative to the phenyl chalcone substrate systematically drives the pseudo-first-order coupling process toward maximum conversion efficiency without impacting the overall rate constant values, aligning with standard empirical observations in chromophore synthesis protocols [12].

   The experimental half-life values calculated in this work—decreasing from 13.1 minutes at 275 K down to 11.3 minutes at 305 K—confirm that the rate of azo-chalcone dye formation accelerates systematically with thermal activation. These kinetic intervals and numerical trends are in identical agreement with previously documented investigations on the kinetics of reactions that lead to colored Azo-Schiff complexes [36, 37].validating the reliability of the integration method utilized to monitor the colored dye formation process.

CONCLUSIONS

1. The azo-chalcone dye formation follows pseudo-first-order kinetics under the studied conditions.
2. The optimum stoichiometric ratio was reported as 1:10 (0.5 mL of 10^{-3} M chalcone solution to 5.0 mL of 10^{-3} M diazotized reagent).
3. The rate constant increased with temperature, reaching the highest value at 305 K (0.0616 min^{-1}) and the lowest value at 275 K (0.0529 min^{-1}).
4. The half-life decreased as temperature increased, indicating faster dye formation at higher temperatures.
5. Arrhenius analysis showed a strong linear correlation ($r^2 = 0.9999$), supporting the temperature dependence of the reaction rate and allowing the calculation of the activation energy.
6. DFT calculations supported the experimental observations and indicated that nitrogen and oxygen donor atoms act as the main active sites in the azo-chalcone molecule

Acknowledgments

The author thanks the Department of Chemistry, College of Education for Pure Science at the University of Mosul for the administrative and technical support during the experimental and computational stages of this work.

Authors' contributions

The author is solely responsible for all aspects of this research, including the experimental work, theoretical calculations, and manuscript writing.

REFERENCES

1. Sweeting, S.G., et al., *The solubility and stability of heterocyclic chalcones compared with trans-chalcone.* Structural Science, 2020. **76**(1): p. 13-17.
2. v. Kostanecki, S. and J. Tambor, *Ueber die sechs isomeren Monooxybenzalacetophenone (Monooxychalkone).* Berichte der deutschen chemischen Gesellschaft, 1899. **32**(2): p. 1921-1926.
3. Sharma, V., V. Kumar, and P. Kumar, *Heterocyclic chalcone analogues as potential anticancer agents.* Anticancer Agents in Medicinal Chemistry (Formerly Current Medicinal Chemistry-Anti-Cancer Agents), 2013. **13**(3): p. 422-432.
4. Yadav, N., et al., *Antimalarial activity of newly synthesized chalcone derivatives in vitro.* Chemical biology & drug design, 2012. **80**(2): p. 340-347.
5. Sharma, N., et al., *Design, economical synthesis and antiplasmodial evaluation of vanillin derived allylated chalcones and their marked synergism with artemisinin against chloroquine resistant strains of Plasmodium falciparum.* European Journal of Medicinal Chemistry, 2014. **79**: p. 350-368.
6. Guantai, E.M., et al., *Enone–and chalcone–chloroquinoline hybrid analogues: in silico guided design, synthesis, antiplasmodial activity, in vitro metabolism, and mechanistic studies.* Journal of medicinal chemistry, 2011. **54**(10): p. 3637-3649.
7. Mishra, N., et al., *synthesis of novel substituted 1, 3-diaryl propenone derivatives and their antimalarial activity in vitro.* European journal of medicinal chemistry, 2008. **43**(7): p. 1530-1535.
8. Valla, A., et al., *New syntheses and potential antimalarial activities of new 'retinoid-like chalcones'.* European journal of medicinal chemistry, 2006. **41**(1): p. 142-146.
9. Rammohan, A., et al., *Chalcone synthesis, properties and medicinal applications: a review.* Environmental Chemistry Letters, 2020. **18**(2): p. 433-458.
10. Sreevidya, T.V., B. Narayana, and H.S. Yathirajan, *Synthesis and characterization of some chalcones and their cyclohexenone derivatives.* Central European Journal of Chemistry, 2010. **8**(1): p. 174.
11. Al Zahrani, N.A., et al., *synthesis of novel chalcone-based phenothiazine derivatives as antioxidant and anticancer agents.* Molecules, 2020. **25**(19): p. 4566.
12. Dhar, R., et al., *2', 4-Dihydroxy-3', 4', 6'-trimethoxychalcone from Chromolaena odorata possesses anti-inflammatory effects via inhibition of NF-κB and p38 MAPK in lipopolysaccharide-activated RAW 264.7 macrophages.* Immunopharmacology and immunotoxicology, 2018. **40**(1): p. 43-51.
13. Rossi, G. and J. Avellino, *An evaluation of the antihistaminic activity of a new series of chalcone derivatives.* American journal of pharmacy and the sciences supporting public health, 1957. **129**(9): p. 324-331.
14. Gan, F.-F., et al., *Novel dual-targeting anti-proliferative dihydrotriazine-chalcone derivatives display suppression of cancer cell invasion and inflammation by inhibiting the NF-κB signaling pathway.* Food and chemical toxicology, 2018. **116**: p. 238-248.
15. Hsieh, C.-Y., et al., *Design and synthesis of benzimidazole-chalcone derivatives as potential anticancer agents.* Molecules, 2019. **24**(18): p. 3259.
16. Khanapure, S., et al., *Anticancer activity of ruthenocenyl chalcones and their molecular docking studies.* Journal of Molecular Structure, 2018. **1173**: p. 142-147.

17. Saeed, N. H., Ali, R. T., & Saied, S. M. (2025). Computational study on the Estramustine (EMCYT) and its active metabolites anticancer drugs 17-α-estradiol and nornitrogen. *Results in Chemistry*, 102747.

18. Benouda, H., et al., *synthesis of a series of chalcones and related flavones and evaluation of their antibacterial and antifungal activities.* Letters in Drug Design & Discovery, 2019. **16**(1): p. 93-100.

19. Monga, V., et al., *synthesis and evaluation of new chalcones, derived pyrazoline and cyclohexenone derivatives as potent antimicrobial, antitubercular and antileishmanial agents.* Medicinal chemistry research, 2014. **23**(4): p. 2019-2032.

20. Bandgar, B.P., et al., *Synthesis and biological evaluation of simple methoxylated chalcones as anticancer, anti-inflammatory and antioxidant agents.* Bioorganic & medicinal chemistry, 2010. **18**(3): p. 1364-1370.

21. Al Ajelly, H.M.S., *The Pharmaceutical Prof le of Oxazine Compound Derived from Chalcones.* Am J Pharmacol Ther, 2021. **5**(1): p. 006-008.

22. Arbeloa, F.L., et al., *Handbook of advanced electronic and photonic materials and devices.* HS Nalwa (Ed.), 2001. **7**.

23. Al Hammouri, S., *Synthesis and Biological Evaluation of Chalcones, Isoxazole and Pyrazole Derivatives Attached with Adamantyl Substituent.* 2019.

24. Ibrahim-Ouali, M. and F. Dumur, *Steroidal chalcones and derivatives: A review.* ARKIVOC-Online Journal of Organic Chemistry, 2022. **2021**.

25. Rao, C.M., et al., *synthesis, characterization and anti microbial activity of novel chalcones and its di hydro pyrimidinenones.* International journal of life science and pharma research, 2015. **5**(3): p. P13-P16.

26. Uwakwe, K., et al., *Molecular dynamics simulations and quantum chemical calculations for the adsorption of some imidazoline derivatives on iron surface.* Global Journal of Pure and Applied Sciences, 2017. **23**(1): p. 69-80.

27. Ikeuba, A.I., et al., *Review of computational methods used in the evaluation corrosion inhibition of metallic materials.* Discover Chemical Engineering, 2024. **4**(1): p. 28.

28. Azzouz, A. and A. Obed Agha, *The influence of surfactants and solvents on the stability constant value of some azo dyes formation between oximes and the diazotized Sulphanilic acid salt.* Journal of Education and Science, 2005. **17**(2): p. 10-16.

29. Hawaiz, F.E., D.J. Raheem, and M.K. Samad, *Synthesis and Characterization of Some New Azoimine Dyes and their Applications.* Synthesis and Characterization of Some New Azoimine Dyes and their Applications, 2016. **18**.

30. Özkınalı, S., M.S. Çavuş, and B.U. Sakin, *synthesis, characterisation and DFT calculations of azo-imine dyes.* Journal of the Turkish Chemical Society Section A: Chemistry, 2018. **5**(1): p. 159-178.

31. Al-Marsumi, A. and M. Al-Niemi, *Determination of thermodynamic parameters and studying the stability of some aromatic complexes derived from 4-dimethyl aminobenzaldehyde with dinitro aniline reagent.* EDITORIAL BOARD, 2021. **16**(2-3): p. 19.

32. Ali Mohsin, A.H., H. Al-Niemi, and M. Mahmoud, *Thermodynamic study for the stability of aromatic complexes formation derived from the reaction of 4-dimethyl amino benzaldehyde with diazotized dinitro aniline reagents.* Egyptian Journal of Chemistry, 2022. **65**(2): p. 421-437.

33. Kshash, A.H., *Synthesis and Characterization of Novel Nitroaniline-Based Azo Compounds as Acid-Base Indicators.* Iraqi Journal for Applied Science, 2025. **2**(4): p. 18-29.

34. Mohammed Abdulrazaq Mahdy, & Noor H. M. Saeed. (2025). A comparative study of the theoretical and practical values of ionization constants for amino acid derivatives in the neutral and anionic states. *Applied Chemical Engineering*, *8*(4), ACE-5796. https://doi.org/10.59429/ace.v8i4.5796

35. Al-Ghouti, M., et al., *Thermodynamic behaviour and the effect of temperature on the removal of dyes from aqueous solution using modified diatomite: a kinetic study.* Journal of Colloid and Interface Science, 2005. **287**(1): p. 6-13.

36. Hasb, A. M., & Saeed, N. H. (2025). Chlorination of n-benzoyl valine by sodium n-chloro-para-toluene sulfonyl amide (cat) hydrochloric acidic: a kinetic and mechanism study. *Kimya Problemleri*, *23*(2), 239-248.

37. Bernasconi, C.F., M.L. Ragains, and S. Bhattacharya, *Reactions that generate aromatic molecules: is aromatic stabilization less or more advanced than bond changes at the transition state? Kinetic and thermodynamic acidities of rhenium carbene complexes.* Journal of the American Chemical Society, 2003. **125**(40): p. 12328-12336.

38. Reeves, R. and L. Tong, *Kinetics of Reaction of Nucleophilic Reagents with Naphthoquinone Imine Dyes in Alkaline Solution.* Journal of the American Chemical Society, 1962. **84**(11): p. 2050-2057.

39. Maqbool, T., P. Srikiratiwong, and H.S. Fogler, *Effect of temperature on the precipitation kinetics of asphaltenes.* Energy & fuels, 2011. **25**(2): p. 694-700.

40. Al-Niemi, H. and M. Mahmoud, *Kinetic Study for the reactions of paracetamol with diazotized (P-nitroaniline & sulfanilic acid sodium salt) reagents.* Egyptian Journal of Chemistry, 2023. **66**(2): p. 535-542.

41. Mohammed, I.Y. and I.K. Jassism, *Synthesis of New Heterocyclic Polymers from Chalcone.* Iraqi National Journal of Chemistry, 2017. **17**(1).

42. Ahmed, N. and H. Ridha, *Synthesis of Some New Chalcone Compounds Derived From (Phenyl Quinoxaline Methyl Benzotriazol) of an Expected Biological Activity.* Journal of Education and Science, 2019. **28**(2): p. 1.0-22.0.

43. Mwene-Mbeja, T.M., *Chemical stability of pharmaceutical organic compounds.* Am. J. Biomed. Sci. Res, 2019. **6**: p. 14-22.

44. Dong, J., et al., *Determination of the half-life of 161Tb.* Applied Radiation and Isotopes, 2023. **193**: p. 110647.

45. Kiraci, A. and H. Yurtseven, *Temperature dependence of the Raman frequency, damping constant and the activation energy of a soft-optic mode in ferroelectric barium titanate.* Ferroelectrics, 2012. **432**(1): p. 14-21.

46. Terracciano, A.C., et al., *Effect of catalytically active Ce0. 8Gd0. 2O1. 9 coating on the heterogeneous combustion of methane within MgO stabilized ZrO2 porous ceramics.* Combustion and Flame, 2017. **180**: p. 32-39.

47. Jensen, F., *Activation energies and the Arrhenius equation.* Quality and Reliability Engineering International, 1985. **1**(1): p. 13-17.

48. Balachandran, V., A. Lakshmi, and A. Janaki, *Ab initio, DFT, HOMO–LUMO and Natural Bond Orbital analyses of the electronic structure of 2-mercapto-1-methylimidazole.* Journal of Molecular Structure, 2011. **1006**(1-3): p. 395-401.

49. Sebastian, S., et al., *Study on conformational stability, molecular structure, vibrational spectra, NBO, TD-DFT, HOMO and LUMO analysis of 3, 5-dinitrosalicylic acid by DFT techniques.* Spectrochimica Acta Part A: Molecular and Biomolecular Spectroscopy, 2015. **136**: p. 1107-1118.

50. Puzzarini, C., J.F. Stanton, and J. Gauss, *Quantum-chemical calculation of spectroscopic parameters for rotational spectroscopy.* International Reviews in Physical Chemistry, 2010. **29**(2): p. 273-367.

Figure (1): Kinetics of the absorption for the produced colored Azo-Chalcone- dye (14NP3PP2E1O+ D4ABzA) versus time.

Figure (2): Application of Arrhenius equation colored Azo-Chalcone-dye (14NP3PP2E1O+ D4ABzA) at natural pH and at λ_{max}=346nm.

1. Sweeting, S.G., et al., *The solubility and stability of heterocyclic chalcones compared with trans-chalcone.* Structural Science, 2020. 76(1): p. 13-17.
2. v. Kostanecki, S. and J. Tambor, *Ueber die sechs isomeren Monooxybenzalacetophenone (Monooxychalkone).* Berichte der deutschen chemischen Gesellschaft, 1899. 32(2): p. 1921-1926.
3. Sharma, V., V. Kumar, and P. Kumar, *Heterocyclic chalcone analogues as potential anticancer agents.* Anti-Cancer Agents in Medicinal Chemistry (Formerly Current Medicinal Chemistry-Anti-Cancer Agents), 2013. 13(3): p. 422-432.
4. Yadav, N., et al., *Antimalarial activity of newly synthesized chalcone derivatives in vitro.* Chemical biology & drug design, 2012. 80(2): p. 340-347.
5. Sharma, N., et al., *Design, economical synthesis and antiplasmodial evaluation of vanillin derived allylated chalcones and their marked synergism with artemisinin against chloroquine resistant strains of Plasmodium falciparum.* European Journal of Medicinal Chemistry, 2014. 79: p. 350-368.
6. Guantai, E.M., et al., *Enone–and chalcone–chloroquinoline hybrid analogues: in silico guided design, synthesis, antiplasmodial activity, in vitro metabolism, and mechanistic studies.* Journal of medicinal chemistry, 2011. 54(10): p. 3637-3649.
7. Mishra, N., et al., *Synthesis of novel substituted 1, 3-diaryl propenone derivatives and their antimalarial activity in vitro.* European journal of medicinal chemistry, 2008. 43(7): p. 1530-1535.
8. Valla, A., et al., *New syntheses and potential antimalarial activities of new 'retinoid-like chalcones'.* European journal of medicinal chemistry, 2006. 41(1): p. 142-146.
9. Rammohan, A., et al., *Chalcone synthesis, properties and medicinal applications: a review.* Environmental Chemistry Letters, 2020. 18(2): p. 433-458.
10. Sreevidya, T.V., B. Narayana, and H.S. Yathirajan, *Synthesis and characterization of some chalcones and their cyclohexenone derivatives.* Central European Journal of Chemistry, 2010. 8(1): p. 174.
11. Rossi, G. and J. Avellino, *An evaluation of the antihistaminic activity of a new series of chalcone derivatives.* American journal of pharmacy and the sciences supporting public health, 1957. 129(9): p. 324-331.
12. Gan, F.-F., et al., *Novel dual-targeting anti-proliferative dihydrotriazine-chalcone derivatives display suppression of cancer cell invasion and inflammation by inhibiting the NF-κB signaling pathway.* Food and chemical toxicology, 2018. 116: p. 238-248.
13. Hsieh, C.-Y., et al., *Design and synthesis of benzimidazole-chalcone derivatives as potential anticancer agents.* Molecules, 2019. 24(18): p. 3259.
14. Khanapure, S., et al., *Anticancer activity of ruthenocenyl chalcones and their molecular docking studies.* Journal of Molecular Structure, 2018. 1173: p. 142-147.
15. Wan, Z., et al., *Synthesis, antiviral bioactivity of novel 4-thioquinazoline derivatives containing chalcone moiety.* Molecules, 2015. 20(7): p. 11861-11874.
16. Benouda, H., et al., *Synthesis of a series of chalcones and related flavones and evaluation of their antibacterial and antifungal activities.* Letters in Drug Design & Discovery, 2019. 16(1): p. 93-100.
17. Monga, V., et al., *Synthesis and evaluation of new chalcones, derived pyrazoline and cyclohexenone derivatives as potent antimicrobial, antitubercular and antileishmanial agents.* Medicinal chemistry research, 2014. 23(4): p. 2019-2032.
18. Bandgar, B.P., et al., *Synthesis and biological evaluation of simple methoxylated chalcones as anticancer, anti-inflammatory and antioxidant agents.* Bioorganic & medicinal chemistry, 2010. 18(3): p. 1364-1370.
19. Al Ajelly, H.M.S., *The Pharmaceutical Prof le of Oxazine Compound Derived from Chalcones.* Am J Pharmacol Ther, 2021. 5(1): p. 006-008.
20. Arbeloa, F.L., et al., *Handbook of advanced electronic and photonic materials and devices.* HS Nalwa (Ed.), 2001. 7.
21. Al Hammouri, S., *Synthesis and Biological Evaluation of Chalcones, Isoxazole and Pyrazole Derivatives Attached with Adamantyl Substituent.* 2019.
22. Ibrahim-Ouali, M. and F. Dumur, *Steroidal chalcones and derivatives: A review.* ARKIVOC-Online Journal of Organic Chemistry, 2022. 2021.

23. Rao, C.M., et al., *Synthesis, characterization and anti microbial activity of novel chalcones and its di hydro pyrimidinenones.* International journal of life science and pharma research, 2015. 5(3): p. P13-P16.
24. Uwakwe, K., et al., *Molecular dynamics simulations and quantum chemical calculations for the adsorption of some imidazoline derivatives on iron surface.* Global Journal of Pure and Applied Sciences, 2017. 23(1): p. 69-80.
25. Ali Mohsin, A.H., H. Al-Niemi, and M. Mahmoud, *Thermodynamic study for the stability of aromatic complexes formation derived from the reaction of 4-dimethyl amino benzaldehyde with diazotized dinitro aniline reagents.* Egyptian Journal of Chemistry, 2022. 65(2): p. 421-437.
26. Meng, G., et al., *Modular click chemistry libraries for functional screens using a diazotizing reagent.* Nature, 2019. 574(7776): p. 86-89.
27. Mohammed, H.A., K.S. Ahmed, and S.I. Hamadamin, *Kinetics and Thermodynamic Studies of the Iodination of Sultams Using A Spectroscopic Technique.*
28. Balachandran, V., A. Lakshmi, and A. Janaki, *Ab initio, DFT, HOMO–LUMO and Natural Bond Orbital analyses of the electronic structure of 2-mercapto-1-methylimidazole.* Journal of Molecular Structure, 2011. 1006(1-3): p. 395-401.
29. Sebastian, S., et al., *Study on conformational stability, molecular structure, vibrational spectra, NBO, TD-DFT, HOMO and LUMO analysis of 3, 5-dinitrosalicylic acid by DFT techniques.* Spectrochimica Acta Part A: Molecular and Biomolecular Spectroscopy, 2015. 136: p. 1107-1118.
30. Puzzarini, C., J.F. Stanton, and J. Gauss, *Quantum-chemical calculation of spectroscopic parameters for rotational spectroscopy.* International Reviews in Physical Chemistry, 2010. 29(2): p. 273-367.
31. Al-Ghouti, M., et al., *Thermodynamic behaviour and the effect of temperature on the removal of dyes from aqueous solution using modified diatomite: a kinetic study.* Journal of Colloid and Interface Science, 2005. 287(1): p. 6-13.
32. Reeves, R. and L. Tong, *Kinetics of Reaction of Nucleophilic Reagents with Naphthoquinone Imine Dyes in Alkaline Solution.* Journal of the American Chemical Society, 1962. 84(11): p. 2050-2057.
33. Maqbool, T., P. Srikiratiwong, and H.S. Fogler, *Effect of temperature on the precipitation kinetics of asphaltenes.* Energy & fuels, 2011. 25(2): p. 694-700.
34. Al-Niemi, H. and M. Mahmoud, *Kinetic Study for the reactions of paracetamol with diazotized (P-nitroaniline & sulfanilic acid sodium salt) reagents.* Egyptian Journal of Chemistry, 2023. 66(2): p. 535-542.
35. Mohammed, I.Y. and I.K. Jassism, *Synthesis of New Heterocyclic Polymers from Chalcone.* Iraqi National Journal of Chemistry, 2017. 17(1).
36. Yeğiner, G., et al., *Transition metal (II) complexes with a novel azo-azomethine Schiff base ligand: Synthesis, structural and spectroscopic characterization, thermal properties and biological applications.* Journal of fluorescence, 2017. 27(6): p. 2239-2251.
37. Elbadawy, H.A., et al., *Synthesis, characterization, computational and dyeing behavior of Cu (II) and Zn (II) metal complexes derived from azo-Schiff bases containing phenol derivatives.* BMC chemistry, 2025. 19(1): p. 207.